

Study of Corrosion-Induced Failure Mechanisms of Epoxy Coated Reinforcing Steel (Parts I and II)

Seung-Kyoung Lee

ABSTRACT

Epoxy coated reinforcing steels (ECRs) were acquired from ten sources and coatings from each source were initially characterized in terms of defects, thickness, solvent extraction weight loss and hardness. Testing involved exposure in three aqueous solutions at elevated temperature (80°C) and in chloride-contaminated concrete slabs under outdoor exposure. It was found that the density and size of coating defects was the primary factor affecting ECR performance. The equivalent circuit analysis using electrochemical impedance spectroscopy (EIS) data indicated that the impedance response for well-performing ECR specimens showed no signs of active degradation at the interface although diffusional processes similar to those noted for poorly performing bars occurred here. Experimental results also indicated a relationship between corrosion behavior and bar source. Weight loss upon solvent extraction correlated with impedance reduction from hot water exposure. Coating defects developed during most of the tests, especially in high pH solutions containing chloride ions. ECRs with excessive coating defects, either initially present or ones which developed in service, performed poorly in every test category regardless of source. Forms of coating failure were extensive rusting at defects, blistering, wet adhesion loss, cathodic delamination, underfilm corrosion and coating cracks. These occurred sequentially or concurrently, depending on the condition of the ECR and nature of the environment.

INTRODUCTION

Premature deterioration of concrete structures caused by corrosion of embedded reinforcing steel has been a serious and costly problem for infrastructure in the United States. According to 1991 U.S. Department of Transportation study, 39 percent of the 576,665 bridges on Interstate, arterials and collector roads are structurally deficient or functionally obsolete [1]. Another report from the Federal Highway Administration (FHWA) in the same year showed that the cost for bridge repair and replacement is expected to rise to about \$4.2 billion per year increased from \$3.5

billion per year estimated for 1991 just to keep up with the rate of deterioration [2]. Chloride contamination has been recognized as the major cause of steel corrosion in concrete, and the service life of concrete structures is shortened accordingly. Where the risk of chloride-induced corrosion exists or where chloride penetration cannot be controlled, use of epoxy coated reinforcing steel (ECR) intends to reduce or eliminate damage to concrete structures by isolating the reinforcing steel from chloride ions by means of powder epoxy coating. Based on the positive results from early research conducted by the National Bureau of Standards (currently National Institute for Standards and Technology) [4] and FHWA [5], powdered epoxy coated reinforcing steel has been widely used.

Dept. of Ocean Engineering, Florida
Atlantic Univ., Boca Raton, FL 33431

Beginning in 1986, however, corrosion of ECR was observed upon various substructure members of bridges in the Florida. These were built approximately thirteen years ago, and premature failure took place after only seven years of service life [6 - 8]. Corrosion was initially observed in the splash zone of the substructures at locations of bent ECRs, but later straight ECRs were found to be deteriorated too. Other cases of unsatisfactory performance of ECR can be found elsewhere [9]. The Technical Research Centre of Finland has also reported that, while some ECRs performed well, others actually had increased rates of corrosion compared to uncoated bars [10]. Because ECR is a new technology with a relatively short history, unexpectedly poor performance of ECR in concrete for some service situations has led to research to identify the exact mechanisms of failure. This study, which utilized experimental and analytical approaches, is a part of such efforts.

EXPERIMENTAL

The ECR specimens were acquired from ten sources (designated as **A, B, C, D, E, F, J, N, T, and U**) including two foreign sources. ECRs from each source were characterized by coating thickness, hardness, defect density and weight loss by solvent extraction method employing hot methyl ethyl ketone (MEK) solution. As a short-term laboratory testing, hot water tests (HWT) were performed with ECR specimens exposed to elevated temperature (80°C) test solutions such as distilled water (DW), 3.5 weight percent NaCl solution (NaCl) and simulated pore water with KCl (SP w/KCl). Periodic EIS scans were performed to monitor the changes of impedance with immersion time for 14 days. At the end of the test

adhesion strength of the coating was determined by a direct pull-off test.

In order to study ECR performance in concrete environment, a total number of 168 ECRs were embedded in 76 test slabs containing chlorides, and the slabs were exposed to natural outdoor weathering with four different wet-dry cycles. Periodic open circuit potential (OCP) and macrocell current measurements were made during exposure period. At certain intervals EIS scanning was performed on selected slab specimens. Autopsies of eight test slabs was performed after ten months of exposure. Some of EIS data obtained from each test category were analyzed by an equivalent circuit model curve fitting technique, and the ECR degradation processes in terms of impedance response were established.

TEST RESULTS AND DISCUSSION

1. Results of coating thickness measurement indicated that regardless of source the coating at the top portion of lug deformations was thicker than the area between the deformations, and the base of rib deformations was the thinnest, as shown in Figure 1. However, the average coating thickness in the valleys for all ECR specimens conformed to the current ASTM specification. For coating hardness, virgin ECRs from eight sources exhibited HB pencil hardness, while ECRs from the two other sources were softer with hardness of B. ECR specimens autopsied from chloride contaminated concrete slab specimens uniformly exhibited the softest hardness 2B.
2. In addition to bare areas induced by mechanical damage, three types of non-mechanical coating defects were identified on virgin ECRs and categorized according to physical appearance. These were pin-

holes, cracks or embedded burrs. Upon exposure of ECRs, the frequency of defect development was influenced by the nature of the test solution. In general, ECRs having cross deformations or a relatively thin coating were particularly susceptible to defect development in test environments.

3. The most frequent site for cathodic blisters during HWT was at the base of rib deformations where the coating was the thinnest. ECR specimens with relatively large defects tended to develop more cathodic blisters than ones with small defects, especially in chloride containing environments. The high pH of the liquid within blisters was attributed to OH^- produced by the cathodic reaction. For autopsied slab ECR specimens, on the other hand, anodic blisters were concentrated on the lower side of the bars facing the bottom mat. This was probably due to concentration of anodic current on the bar side facing the macro cathode and to electromigration of chloride ions into blisters. Pits were usually found beneath anodic blisters.

4. There was an apparent correlation between coating weight loss in the solvent extraction test and impedance at 0.1 Hz after one day of DW HWT. As shown in Figure 2, the coatings with low weight loss demonstrated low reduction of impedance, whereas high weight loss correlated with a large decrease in impedance for bars that performed poorly during HWTs. This suggested that impedance reduction in HWT was related, at least in part, to the state of coating cure or to presence of soluble fillers.

5. The adhesion strength of virgin epoxy coatings exceeded 64 MPa, but coatings on specimens soaked in hot water environments exhibited adhesion loss. Figure 3 shows that coatings exhibited higher adhesion values after exposure in

hot NaCl and SP w/KCl solutions compared to those tested in hot DW, provided that coating defects were not excessive. This is consistent with osmotic pressure having been higher in DW compared to the salt containing environments. Adhesion recovery of most specimens occurred upon drying. Specimens with high adhesion strength tended to exhibit a relatively large amount of coating residue on the substrate with the trend being more apparent for specimens dried for extended times. Autopsied slab ECR specimens exhibited high adhesion strength compared to ones obtained from HWT unless the coating had deteriorated badly.

6. ECR specimens that performed poorly in concrete exhibited macroscopic coating cracks and anodic blisters with cracks around the base, and underfilm corrosion was extensive in many cases. Furthermore, a cathodically delaminated zone with and without underfilm corrosion could be observed near coating defects, even for ECR specimens with no external indication of such deterioration. For HWT specimens underfilm corrosion formed a ring of rust colored corrosion products around initial defects and cathodic delaminated areas were located beyond the rust layer. DW tended to produce a larger disbonded area than NaCl solution.

7. Figures 4 and 5 show the EIS responses for initially defect-free ECR specimens after 1 day exposure in DW and NaCl HWTs, respectively. According to EIS data analysis, reduction of pore resistance (R_{po}) in HWT was the largest during the first day, and the corresponding coating capacitance (C_c) increased with time. When coatings deteriorated by blistering, new defects and macroscopic coating cracks, high C_c was observed. Interfacial impedance (Z_f) was attributed to either charge transfer

resistance (R_{ct}) and double layer capacitance (C_{dl}) or diffusion, depending on the condition of the ECR and the environment. EIS data from slab ECR specimens contained a diffusion response more often than did specimens tested hot water environments, indicating that the degradation process of ECRs in concrete was, in many cases, diffusion control. Some slab EIS data exhibited an additional diffusion response at intermediate frequencies. This might suggest that diffusion through the coating or corrosion products could be another contributing factor to total impedance of the ECR coating system.

8. A total of six equivalent circuit models was established to fit the experimental EIS data, depending on the state of ECR degradation. They are listed in Figure 6. An RC transmission line analog using a constant phase impedance circuit element was employed to model the nonhomogeneous diffusion response. For poorly performing defect-free ECR specimens in HWT, EIS data indicated rapid water and oxygen absorption; These species reached the coating/substrate interface and caused coating degradation; and this process was sometimes controlled by diffusion. This progressive degradation was simulated by four circuit models. For well-performing ECR specimens, the impedance response, in general, showed no signs of active electrochemical reactions but instead a diffusion-related response which might indicate a low rate of corrosion. Since the majority of slab EIS data showed relatively low impedances, circuit models which represented more deteriorated stages were used.

9. Based on the findings in this study, it can be suggested that a short-term accelerated test involving initially defect-free ECRs in various solutions at 80 °C can be utilized as a quality control

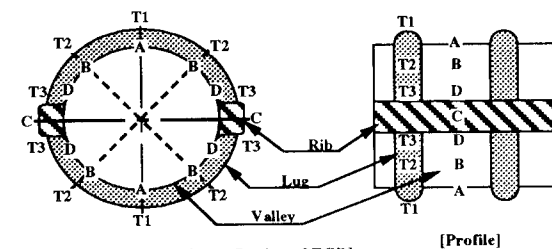
methodology along with the solvent extraction test. If the ECRs perform well in these tests without defect development, retain high R_{po} in hot water environments and possess low solvent extraction weight loss, good performance of ECRs in aggressive environments is highly probable.

REFERENCES

1. ENR Washington Observer, Engineering News Record, Vol. 227, No. 2, July 15, 1991, p. 7.
2. "Subcommittee Leader Pushes Bridge Funding", Engineering News Record, Vol. 226, No. 20, May 20, 1991, pp. 13 - 14.
3. Gustafson, D. P., "Epoxy-Coated Reinforcing Bars - Weapon against Corrosion of Rebars in Concrete", Concrete Construction, November 1983, pp. 826 - 836.
4. Clifton, J. R., Beeghly, H. F. and Mathey, R. G., "Protecting Reinforcing Bars from Corrosion with Epoxy Coatings", Corrosion of Metals in Concrete, ACI SP-49, American Concrete Institute, Detroit, 1975, pp. 115 - 133.
5. Clear, K.C. and Virmani, Y.P., "Corrosion of Non-Specification Epoxy-Coated Rebars in Salty Concrete", Paper No. 114, presented at CORROSION/83, April 18 - 22, 1983, Anaheim, California.
6. Gustafson, D.P., "Epoxy Update", Civil Engineering, American Society of Civil Engineers, Vol. 58, No. 10, October 1988, pp. 38 - 41.
7. Zayed A. M., Sagues, A. A. and Powers, R., "Corrosion of Epoxy-Coated Reinforcing Steel in Concrete", Paper No. 379, presented at CORROSION/89, April 17 -21 1989, New Orleans, Louisiana.
8. Sagues, A. A., Powers, R. and Zayed, A. M., "Marine Environment Corrosion of Epoxy-Coated

Reinforcing Steel", Proceedings, 3rd International Symposium on Corrosion of Reinforcement in Concrete Construction, Society of Chemical Industry, May 1990, Wishaw, North Warwickshire, UK.

9. "Performance of Epoxy-Coated Reinforcing Steel in Highway Bridges", Final Report submitted to National Cooperative Highway Research Program Project No. 10-37 by K. C. Clear, Inc. and Florida Atlantic University, July 29, 1994.
10. Ridout, G, "Warnings Sounded on Coated Reinforcement", Building Technical File, No. 28, January 1990, pp. 5 - 7.



[Definition of Notation: Cross-Section of ECR]

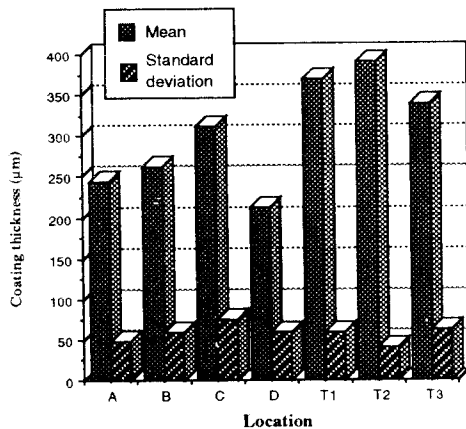


Figure 1. Variation of Average Coating Thickness of ECRs from Ten Sources at Different Geometric Locations.

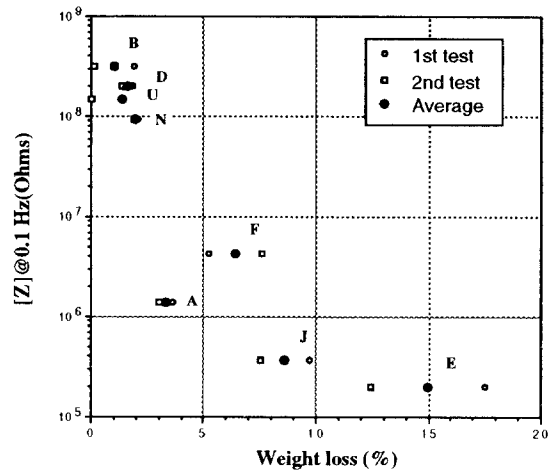


Figure 2. Relationship between Solvent Extraction Weight Loss and [Z] at 0.1 Hz after One Day in DW HWT.

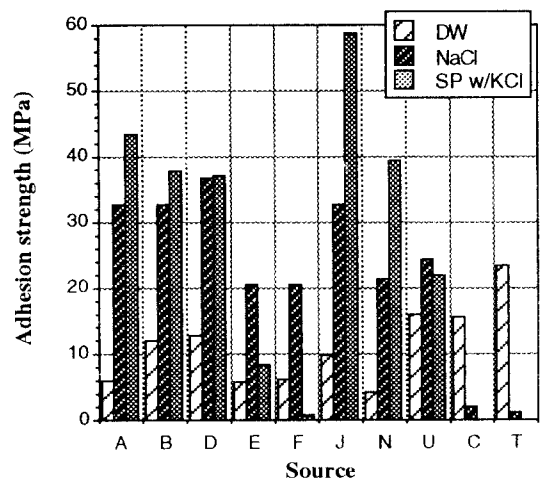


Figure 3. Average Adhesion Strength of ECR Specimens Previously Exposed to Different HWTs (One Day of Drying).

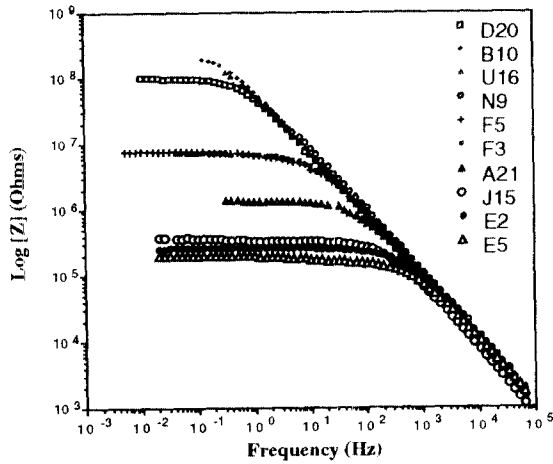


Figure 4. Bode Magnitude Plot for Initially Defect-Free Specimens Obtained after One Day in DW HWT.

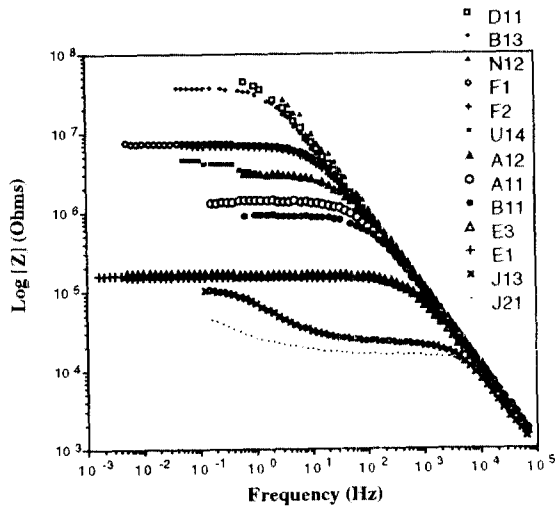


Figure 5. Bode Magnitude Plots for Initially Defect-Free Specimens Obtained after One Day in NaCl HWT.

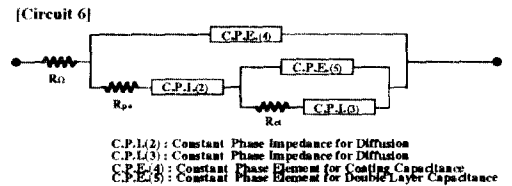
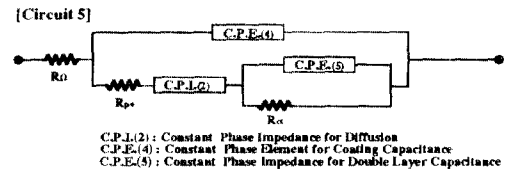
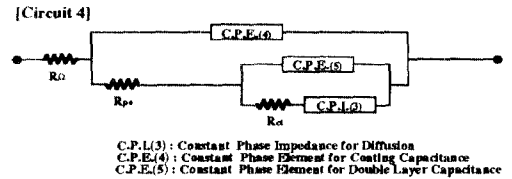
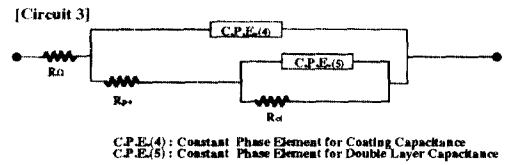
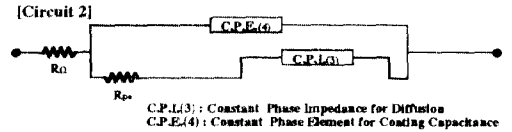
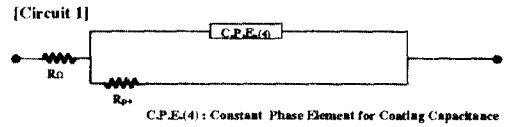


Figure 6. Equivalent Circuit Models.